NEUTRINO PRODUCTION OF DIMUONS

K. Lang, A. Bodek, F. Borcherding,
N. Giokaris, I.E. Stockdale

University of Rochester, Rochester, NY 14627

P. Auchincloss, R. Blair, C. Haber, S. Mishra,
M. Ruiz, F.J. Sciulli, M. Shaevitz,
W.H. Smith, R. Zhu

Columbia University, New York, NY 10027

Y.K. Chu, D.B. MacFarlane, R.L. Messner,
D.B. Novikoff, M.V. Purohit

California Institute of Technology,
Pasadena, CA 91125

R. Coleman, H.E. Fisk, Y. Fukushima, Q. Kerns,
B. Jin, D. Levinthal, T. Kondo, W. Marsh, P.A. Rapidis,
S. Segler, R. Stefanski, D. Theriot,
H.B. White, D. Yovanovitch

Fermi National Accelerator Laboratory,
Batavia, IL 60510

O. Fackler, K. Jenkins

Rockefeller University, New York, NY 10021

Talk presented by Wesley H. Smith.

ABSTRACT

A sample of 493 ν and 41 $\bar{\nu}$ produced opposite sign dimuons with a momentum, $P_\mu > 4$ GeV/c and a sample of 18 same sign dimuons with $P_\mu > 9$ GeV/c are presented. Evidence for a prompt origin of same sign dimuons is discussed. The opposite sign dimuons are used to extract information about neutrino production of charm including cross section, fragmentation, the amount of strange sea, and the Kobayashi Maskawa angle θ_2.

INTRODUCTION

The dimuon data come from two runs with the same detector using the Fermilab narrow band neutrino beam as a neutrino source.[1] The first run (Fermilab experiment E616) took place in 1979 and 1980, with an integrated proton flux of 5.4×10^{18} on the production target. The second run took place in 1982 (Fermilab experiment E701) with a flux of 3.4×10^{18}. Data were taken at six momentum settings for π and K mesons ($+100$, ± 120, ± 140, ± 165, ± 200, ± 250 GeV/c), yielding neutrinos with energies between 40 and 230 GeV. The neutrino beam was produced by decays of these sign and momentum selected ($\Delta P/P = \pm 11\%$) pions and kaons in a 352 m long evacuated decay pipe.

APPARATUS DESCRIPTION

The neutrino detector, shown in Fig. 1, is located in Lab E, 1292 m from the beginning of the decay pipe. The apparatus consists of a target calorimeter instrumented with scintillation counters and spark chambers, followed by an iron toroidal muon spectrometer. The 690 ton target calorimeter is constructed of 168 3m x 3m x 5cm steel plates, 82 3m x 3m liquid scintillation counters (located every 10 cm of steel) and 42 3m x 3m magnetostrictive readout spark chambers (located every 20 cm of steel). For the second run of the experiment, only the downstream two-thirds of the target was used. Minimum ionizing muons were used to maintain the counter gains. The calorimeter was calibrated with a hadron beam of known momentum. The rms hadron energy resolution is $0.89\sqrt{E}$ (GeV).

The muon spectrometer consists of 3 3m long toroidal magnets (containing 1.6m of steel each) with 1.8m outer radius and a 12.7cm radius hole for the

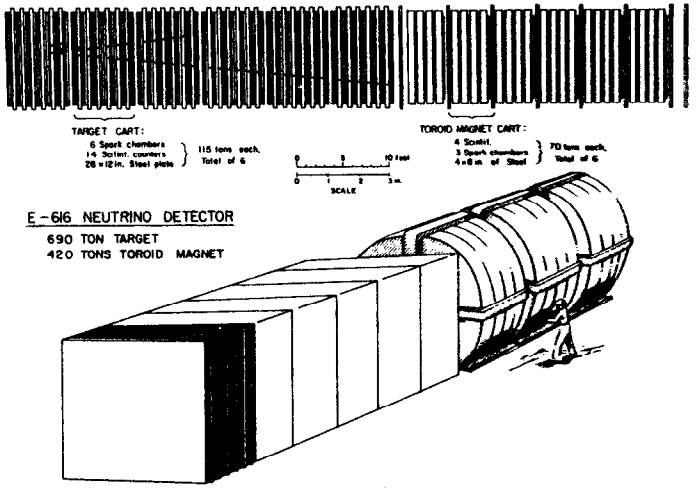

Fig. 1

The CCFRR Detector.

coils. In the first run, the five toroid gaps were instrumented with a combination of 1.5m x 3m and 3m x 3m spark chambers as shown in Fig. 1, along with the larger chambers located downstream. In the second run, only the second and fourth gaps were instrumented with 5 3m x 3m chambers each. The total transverse momentum kick of the toroids is 2.4 GeV/c and the fractional momentum error is 11%.

DIMUON ANALYSIS

Events with two muons were selected from the sample of all charged current events (100K events) which had two or more hits in the downstream target or toroid spark chambers, or at least twice minimum ionizing pulse height in the target or toroid scintillation counters. This computer-selected sample contained one-quarter of the entire charged-current data sample. The selection efficiency for this sample was measured to be (100±2)% by scanning all events in 10% of the data. Events in the computer-selected sample were displayed on a fine resolution graphics terminal to visually select events in which two tracks are present in the spark chambers and scintillation counters. In this way, 2000 legitimate dimuon events were selected. The computer reconstruction of the dimuon events was examined by physicists and, if necessary, selection of hits was performed manually.

Dimuon events must pass the same analysis cuts as the single muon events. Events must have a transverse vertex within a 2.5m x 2.5m square and a longitudinal vertex at least 3.8m from the downstream end of the target, to ensure containment of the hadron shower. At least one muon track must have an angle of less than 200 mrad with respect to the beam axis and its straight line extrapolation from the target must pass through the first toroid magnet, and intersect the trigger counter placed after it. This improves the efficiency for the muon track reconstruction.

Events are separated into those produced by muon neutrinos from pion decay (ν_π) and from kaon decay (ν_K). The neutrino energy and decay angle (and therefore the event radius at the detector) are kinematically related. Events due to ν_K and ν_π are distinguished by examining the transverse radial position of the interaction and the measured total energy. The ν_π event vertex is required to have a transverse radius of less than 76 cm. The final event sample includes 89,667 ν and 8,553 $\bar{\nu}$ charged-current events passing all cuts.

LIKE SIGN DIMUONS

The like sign dimuon sample contains 18 events where each muon traverses one toroidal magnet and has a momentum greater than 9 GeV/c. Both muons are required to pass all the single muon event cuts. However, only one of the muons must satisfy the extrapolation condition to the muon trigger counter. In addition, muons must have fitted tracks which originate in a common vertex consistent with counter pulse height and each track must be visible in the spark chambers after the first toroid.

Principal sources of like sign dimuons are the decay to a muon of a primary π or K at the hadron vertex in a charged-current event and the production of either a prompt or nonprompt muon from the interactions of the primary hadrons in the hadron shower. The inclusive primary hadron spectra and multiplicity are obtained from fits to BEBC ν-Ne[2] and EMC μ-p data.[3] The contribution of subsequent interactions of these hadrons is calculated using the measured prompt and nonprompt muon production by hadrons in the Fermilab experiment E379/595 variable density target.[4] This yields the probability for producing a muon with a momentum,

P_{μ_2}, greater than a particular cutoff value as a function of x_{BJ} and the hadron energy, E_H.

The model of the background uses the unsmeared E_H and x of charged-current Monte Carlo events to generate dimuon events with a particular weight and P_{μ_2}. The produced muon is given a $P_\perp$ based on transverse momentum fits to hadrons from EMC μ-p data.[5] The Monte Carlo events are reconstructed and required to pass the dimuon analysis cuts. The background is normalized to the number of charged current data events passing the same cuts.

There are significant uncertainties in the background calculation. The calculated level of nonprompt muon production depends heavily on the data used to determine it. For first generation decays, we assume ν-Ne distributions are the same as ν-Fe distributions. A survey of neutrino induced final states in bubble chamber experiments and hadronic production in μ-p scattering reveals some differences in the parameters governing hadron fragmentation. The investigation of the background is continuing; at present we estimate the error in the background at 50%.

The background for the 18 events is calculated to be of order half the sample. The present uncertainty in the background calculation leaves in question the existence of a prompt, like sign dimuon signal in these data from absolute rate arguments alone. A resolution of the difficulties mentioned above could improve this significantly. The problem is being worked on. Rates from these data are consistent with preliminary values already reported.[6] CDHS reported 91 ± 9 like sign dimuons with a calculated background of 64 ± 10 events from their 350 GeV wide band run,[7] 47 events with a background of 30 ± 8 from their 200 GeV narrow band run[8] with a momentum cut of 10 GeV/c, and 43 (11) events with a background of 19(3) events from their 300 GeV narrow band run[9] with a momentum cut of 5(10) GeV/c. The CHARM collaboration reported 74 ± 17 prompt ν_μ induced $\mu^-\mu^-$ and 52 ± 13 prompt ν_μ induced $\mu^+\mu^+$ from their wide band run[10] with a 4 GeV/c momentum cut. The HPWFOR collaboration reported a prompt signal of 52 ± 31, 65 ± 15, and 37 ± 11 from their quadrupole triplet run[11] with momentum cuts of 5, 10, and 15 GeV/c, respectively. The CFNRR collaboration reported 12 like sign dimuons with a background of 1.3 events from their quadrupole triplet run.[12] The energy dependence of the rates of prompt, like sign, dimuons to charged-current events is shown in Fig. 2.

Event kinematics may be used to see whether π and K decay can be the sole explanation of the like sign dimuon signal. Distributions of several kinematic variables for the like sign dimuons and the π and K decay background Monte Carlo are shown in Fig. 3. The integral of the background is normalized to that of the data. The distribution of the angle between the two muon tracks projected on a plane perpendicular to the incident neutrino is shown in Fig. 3a. The peaking of this distribution near 180^o indicates that the second muon is associated with the hadron shower in a large fraction of the events. This is a property expected of π and K decay.

For further comparison with the hypothesis of π and K decay the second muon is chosen to be the muon which has the smaller momentum in the direction perpendicular to the axis of the hadron shower ($P_{\perp 2\ min}$). The hadron shower direction is determined from the incoming ν beam properties and the chosen

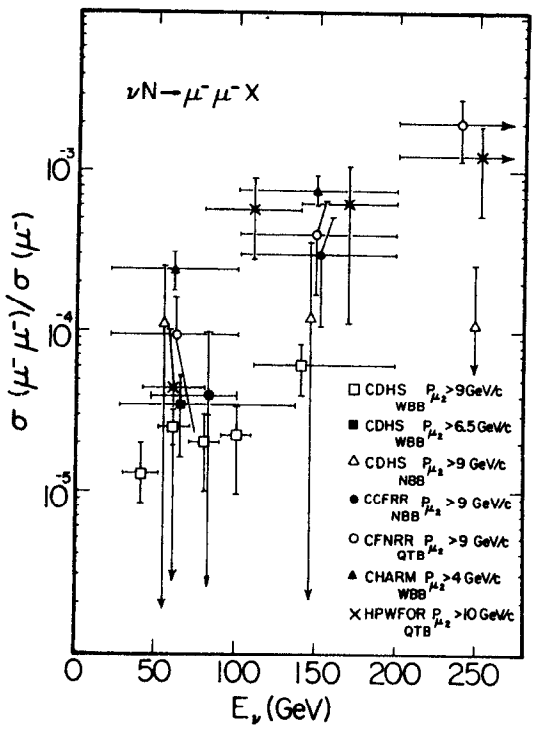

Fig. 2

Like Sign Dimuon Rates vs. E_ν.

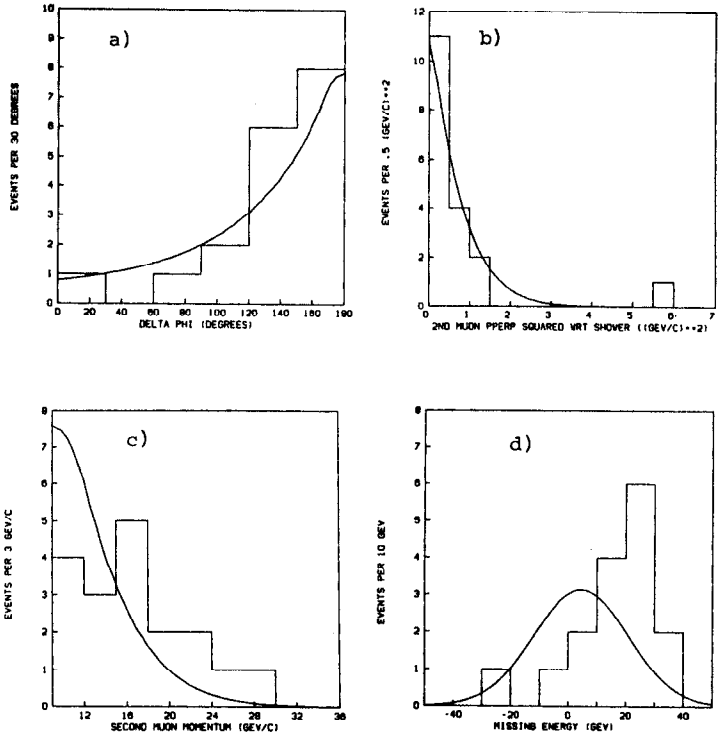

Fig. 3

Distributions of Like Sign Dimuon Data (histogram) and M.C. (curve) Normalized to Data Integral.

first muon. Figure 3b shows the $(P_{\perp 2\ min})^2$ distribution. There is one event with a $(P_{\perp 2\ min})^2$ of 5.9 $(GeV/c)^2$, which is unlikely to be from π and K decay. Figure 3c displays the momentum of the chosen second muon. The average value for the data is (16.8±1.3±0.9)GeV/c where the second error is systematic, and the average value for the background is (12.5±1.0)GeV/c. The data average is 2.3 standard deviations greater than the Monte Carlo. Figure 3d shows the distribution of missing energy for all ν_K events. The missing energy is the difference between the neutrino energy determined by the transverse vertex radius and the measured energy. The determination of missing energy has been verified for single muon events where the average value for ν_K data is (0.66±1.00)GeV and for Monte Carlo is (0.11±0.24)GeV. The like sign,dimuon data have an average missing energy of (15.1±4.2± 1.0)GeV, where the second error is systematic, and the background average is (3.5±0.5)GeV. The missing energy for the data is 2.7 standard deviations greater than that expected for the hypothesis of π and K decay.

Although at present there are some uncertainties in the background rates, even when allowing the background to have the same rate as the like sign dimuon signal, there are several events with kinematics suggesting another source of the observed events.

OPPOSITE SIGN DIMUONS

The opposite sign dimuon event criteria are the same as those for the like sign dimuons with a few exceptions. The ν_K events are required to have a transverse vertex within a 2.5 m radius of the beam center. The angle cut on the second muon is 370 mr. In addition, the muon momentum cut is 4 GeV/c for both muons. While the probability for full momentum reconstruction in the toroids of a muon is low below 9 GeV/c, a lower limit on its momentum can be determined from energy loss by measuring the distance traversed in steel. The 4 GeV/c cut is then a requirement that the muon pass through a distance of 2.9 m in steel. After analysis cuts, there are 493 dimuons produced by neutrinos and 41 from antineutrinos. The calculated π and K decay background is 155±39 for neutrinos and 11±3 for antineutrinos.

Figure 4a shows the ratio $\sigma(2\mu)/\sigma(1\mu)$ corrected for geometric acceptance for the ν induced dimuon signal and its calculated background versus neutrino energy for $P_\mu > 4$ GeV/c. The 2μ background/1μ rate increases linearly with energy and reaches 3×10^{-3} at E_ν = 180 GeV. Figure 4b shows the 2μ/1μ rate for ν induced dimuons after subtraction of the π and K decay background. The prompt 2μ/1μ rate rises to $(5.8\pm0.7) \times 10^{-3}$ at E_ν = 180 GeV. Figure 4c shows this rate for CDHS wide band,[13] CDHS narrow band,[9] and CHARM wide band[14] data. The CDHS measurements require muons to have a track length in their apparatus that is equivalent to a momentum cut between 5 and 6.5 GeV/c. The CHARM measurement places a 4 GeV/c cut on the muon momentum. All experiments agree within errors and show a prompt, opposite sign,dimuon rate of 1/2% of the charged current rate above E_ν of 150 GeV. Figure 4d shows the CCFRR $\bar{\nu}$ rate of $\sigma(2\mu)/\sigma(1\mu)$ versus $E_{\bar{\nu}}$ after subtraction of the π and K decay background.

Experiments in bubble chambers[15] and emulsions[16] have verified that single charm production and decay are the predominant source of the prompt, opposite

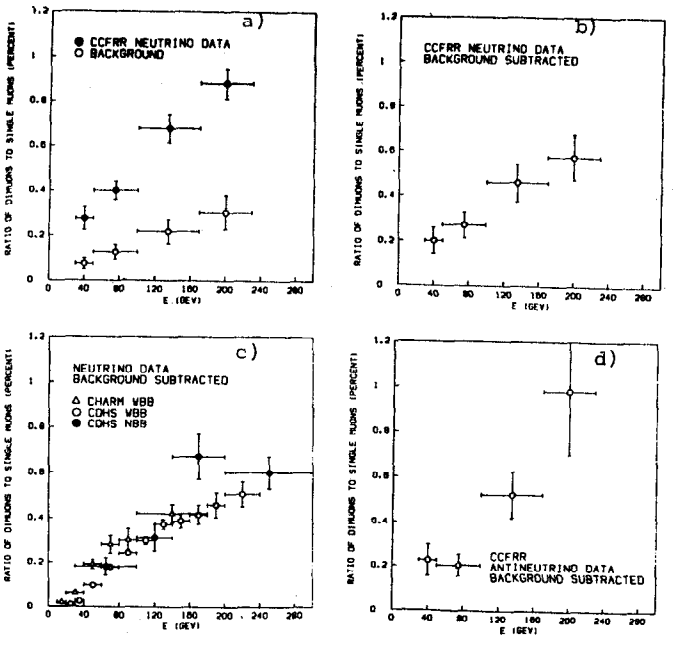

Fig. 4

Energy Dependence of Opposite Sign Dimuon Production.

sign, dimuon signal in neutrino interactions. The rate for production of charm by neutrinos is proportional to $d(x)\sin^2\theta_c + s(x)\cos^2\theta_c$, where θ_c is the Cabbibo angle and $d(x)$ and $s(x)$ are the quark density distributions in the proton. The antineutrino rate is proportional to $\bar{d}(x)\sin^2\theta_c + \bar{s}(x)\cos^2\theta_c$. The neutrino rate has contributions from both valence down quarks and sea strange quarks, while the antineutrino rate is predominantly due to the antistrange sea.

The V-A structure of the weak interaction predicts that neutrino and antineutrino production of charm (in the absence of threshold effects) is uniform in y because it proceeds solely on quarks for neutrinos and antiquarks for antineutrinos. The inclusion of the threshold effect described below causes the y distribution to peak at higher y. To create a charm quark with mass, m_c, the fraction of nucleon momentum carried by the light quark, usually called x, is actually $x'=x+m_c^2/(2ME_H)$. In the calculation of charm production,[17] x' is substituted for x as the appropriate scaling variable and the phase space factor for producing a heavy quark in two body scattering is included. The charmed hadron production differential cross section is then[18]:

$$\frac{d^3\sigma}{dx'dydz} = \frac{\sigma^2 ME_\nu}{\pi}[x'd(x')\sin^2\theta_c + x's(x')\cos^2\theta_c][1-\frac{m_c^2}{2ME_\nu x'}]D(z).$$

The fragmentation function of the charm quark is D(z) where z is the fraction of energy taken by the charm particle (i.e. D meson) in the W boson nucleon c.m.

Neutrino production of charm is simulated with the Monte Carlo calculation described above that uses both

valence and sea x distributions from CCFRR data.[19] The transverse momentum distribution of the charmed mesons with respect to the hadron shower direction is taken to be $e^{-3.1\ p_t}$ from a fit to emulsion data.[16] The charm branching ratio to muons of (7.1±1.3)% is determined from the branching ratio of the mixture of charm particles found in e^+e^- reactions[20] when applied to the composition of charm particles found in the neutrino emulsion data.[16] Finally, the charm quark mass is assumed to be 1.5 GeV/c^2.

Since neutrino counter experiments do not measure z directly, charm fragmentation is studied in the observed distribution of $z' = E_{\mu_2}/(E_H+E_{\mu_2})$ where E_{μ_2} is the energy of the second muon and E_H is the measured energy in the shower. A Monte Carlo fit is made for the form of Peterson et al.[21]: $D(z) \propto 1/[z(1-1/z-\varepsilon/(1-z))^2]$. We find $\varepsilon = 0.40^{+.25}_{-.11}$. CDHS finds the value $\varepsilon = 0.22^{+.11}_{-.08}$.[9] An average of world e^+e^- data[22] on the D^* fragmentation function gives $\varepsilon = 0.29\pm0.04$. The z' distribution for the CCFRR data is shown in Fig. 5 with the fit to the Peterson fragmentation function ($\varepsilon = 0.4$) and the fragmentation $D(z) = \sqrt{z}(1-z)$, which is also a good fit to the data and is the form assumed for the subsequent analysis of the x distributions.

The x distributions of the background subtracted dimuon data for neutrinos and antineutrinos are shown in Fig. 6. Also shown is the charm Monte Carlo calculation. The Monte Carlo uses a strange sea $s(x) = f\cdot\bar{d}(x)$. CDHS finds $f = 0.52 \pm 0.09$.[13] A preliminary fit to f is made with these x distributions using the Monte Carlo. We find $f = 0.70^{+.10}_{-.09}$ (statistical errors only) with χ^2=16.9 for 14 degrees

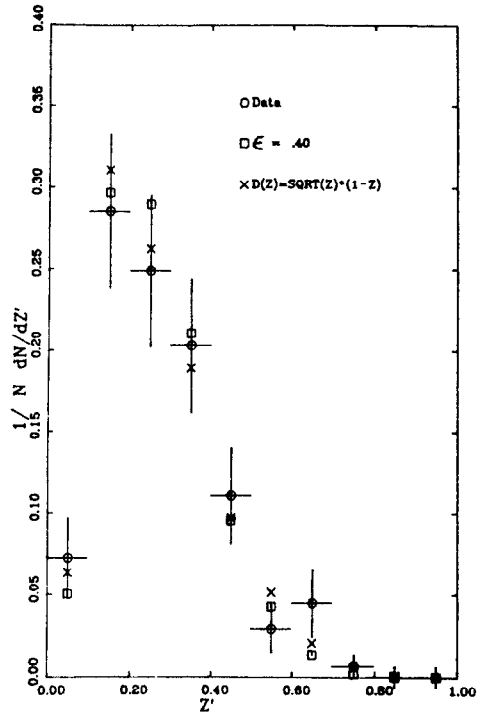

Fig. 5

Dimuon z' Distribution for Background Subtracted Data (circles) and Charm Monte Carlo with the Peterson Fragmentation Function (boxes) and $D(z)=\sqrt{z}(1-z)$ (crosses).

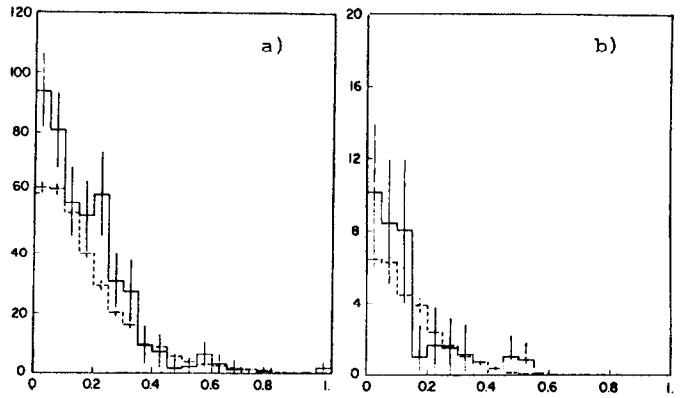

Fig. 6

Number of Dimuon Events vs x for Neutrinos (a) and Antineutrinos (b). The solid line represents background subtracted data and the dashed line the charm Monte Carlo with m_c = 1.5 and s = 1/2 $\bar{d}$.

of freedom. When we include the systematic errors due to the uncertainty in the charm quark mass and leptonic branching ratio, we conclude $f = 0.67^{+.27}_{-.19}$.

In the Kobayashi-Maskawa model, $\sin\theta_c=\sin\theta_1\cos\theta_2$.[23] If the contribution from sea quarks is eliminated, $\sin\theta_c$ is the ratio of $2\mu/1\mu$ cross sections after the effects of the charm threshold, muon momentum cut and branching ratio are removed. To isolate the valence 2μ cross section from the sea contribution, we only use neutrino data for which $x > 0.3$, since the sea quarks are concentrated at low x $(\sim(1-x)^7)$, and the valence is not $(\sim \sqrt{x}(1-x)^3)$. Experiments on β decay and semileptonic hyperon decays determine[21] $\sin\theta_1=0.228\pm0.011$. We therefore find $\cos\theta_2=1.14\pm0.35$. The CDHS group[13] find $\cos\theta_2=1.05\pm0.14$.

CONCLUSIONS

We observe 18 like sign dimuon events. Uncertainties in the π and K decay background make it difficult to conclude at present that there is a definite prompt signal from the absolute rate of this experiment alone. The distributions of momentum perpendicular to the hadron shower direction, second muon momentum and missing energy suggest that the properties of the observed events are different from those expected from π and K decay muons. We observe a prompt opposite sign dimuon signal consistent with the hypothesis of charm production. The rate with respect to single muon events is 5.8×10^{-3} at E_ν=180 GeV for P_μ>4 GeV/c. The charm fragmentation function has been fit to the Peterson form with $\epsilon=0.40^{+.25}_{-.11}$. The best fit value of the strange sea is less than the down sea: $\int dx\bar{s}(x)=(0.67^{+.27}_{-.19})\int dx\bar{d}(x)$. The Kobayashi Maskawa angle θ_2 has been measured to be $\cos\theta_2=1.14\pm.35$.

REFERENCES

1) R. Blair et al., Phys. Rev. Lett. 51, 3431 (1983).
2) P.C. Bosetti et al., Nucl. Phys. B149, 13 (1979); B209, 29 (1982).
3) J.J. Aubert et al., Phys. Lett. 114B, 373 (1982).
4) Fermilab E379/595. (c.f. J. Ritchie, Ph.D. Thesis, U of Rochester (1983) and K.W.B. Merritt, Ph.D. Thesis, Caltech (1981). Data do not exist for $E_\pi < 40$ GeV, where we use a M.C. calculation.
5) F.W. Brasse, in Proc. of XX Int. Conf., Madison, Wisc., p. 755 (1980).
6) H.E. Fisk, Proc. Int. Symp. Leptons & Photons at High Energies, p. 703 (1981).
7) J.G.H. deGroot et al., Phys. Lett. 86B, 103 (1979).
8) M. Holder et al., Phys. Lett. 70B, 396 (1977).
9) B. Renk, Ph.D. Thesis, Dortmund Univ. (1984).
10) M. Jonker et al., Phys. Lett. 107B, 241 (1981).
11) T. Trinko et al., Phys. Rev. D23, 1889 (1981).
12) K. Nishikawa et al., Phys. Rev. Lett. 46, 1555 (1981).
13) H. Abramowicz et al., Z. Phys. C15, 19 (1982).
14) M. Jonker et al., Phys. Lett. 107B, 241 (1981).
15) C. Baltay et al., Phys. Rev. Lett. 41, 73 (1978).
16) N. Ushida et al., Phys. Lett. 121B, 292 (1983).
17) R. Brock, Phys. Rev. Lett. 44, 1027 (1980).
18) B.J. Edwards, T.D. Gottschalk, Nucl. Phys. B186, 309 (1981).
J. Kaplan, F. Martin, Nucl. Phys. B115, 333 (1976).
C.H. Lai, Phys. Rev. D18, 1422 (1978).
19) D. MacFarlane et al., Fermilab PUB-83/108-EXP, submitted to Z. Phys. C (1984).
20) W. Bacino et al., Phys. Rev. Lett. 43, 1073 (1979).
J.M. Feller et al., Phys. Rev. Lett. 45, 329 (1978).
R.H. Shindler et al., Phys. Rev. 24, 78 (1981).
21) C. Peterson et al., Phys. Rev. D27, 105 (1983).
22) J. Chapman, Proc. of the 12th SLAC Summer Institute on Particle Physics (1984).
23) R.E. Shrock, L.L. Wang, Phys. Rev. Lett. 41, 1692 (1978); 42, 1589 (1979).